4. Voltage stability with RE

Voltage stability of trunk system with highly integrated RE accompanied by three-phase-to-ground fault was already reported(1). However, three-phase-to-ground fault hardly occurs in trunk system. Because, some two-phase faults are observed but three-phase fault on 500kV transmission line by lightning strike was not reported. Possible three-phase faults on trunk system are only 1) internal fault of three-phase in one GIS and 2) charging without removing temporary grounding. Here, voltage stability with more frequent failure is assumed, that is, not trunk system but local system, not three-phase fault but simple one circuit trip on double circuit line without any grounding.

For analysis, P-V curve, N-V curve, T-ω curve are used. For simulation, long term voltage calculation program(so called as V method), and RMS stability calculation program (so called Y method) are used.

The 154kV/77kV substation with the worst voltage stability in Hokuriku region is chosen as example system. Load is modeld as 1) static load expressed by index function (usually used in practice), 2) 50% electricity is used by induction motor. Load location is modeled as 1) directly connected to 77kV bus (usually used in practice), 2) load is connected via load branch to 77kV bus.

When RE is highly integrated, its outout is assumed as 0.2 p.u. (at 1GVA base). Voltage sensitivity of RE during low voltage is modeled as 1) constant impedance , 2) constant current.

As analysis results, 1) induction motor load and 2) load branch inpedance are indispensable.

As voltage sensitivity of RE during low voltage, constant current is more favorable than constant impedance forvoltage stability.

Since number ofanalysis cases is large, only indispensable case study resuts are introduced for story progress.

There are two voltage instabilities(1).

The first is ran-away of LTC (on-Load Tap Changer) on transformer, and is called as slow voltage instability.

The second is stall of induction motor load, and is called as “fast voltage instability”.

Many articles on slow voltage instability have been published in Japan. Because, west Kanto blackout occurred in 23 July 1987, and the aspect was explained as slow voltage instability. However, some opinions that “voltage collapse” in which voltage declines very fast cannot be explained by tap operation and modeling induction motor stall is indispensable were published.

On the contrary, number of articles referring fast voltage instability is very small in Japan. The fact must have close relation with the history that induction motor load model has not been adopted for a very long time in power system analysis practice only in Japan among all developed and developing countries.

Existing local load system model

The simplest model for reproducing the two voltage instabilities is shown in Fig. 4.1. A 154kV/77kV substation and feeding line having having the poorest voltage stability in Hokuriku region are taken as example. Fatally important elements only are considered, So, resistance and capacitance on network and resistance of motor’s primary winding is ignored.

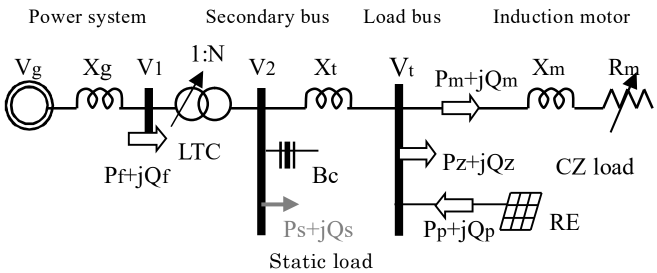

Fig. 4.1 Minimum model for reproducing voltage instabilities

Initial values are shown as follows at 1GVA base when not specially commented.

$V_g = 1.01$,　$X_g = 0.8132$ (two circuits),　1.318 (one circuit)

$X_t = 0.5578$,　$X_m = 0.09$ (at motor consuming power base)

$N = 1$,　$V_2 = 1$,　Bc is adjusted to maintain $V_2 = 1$

Trunk system is expressed as voltage source V_g behind internal reactance X_g. Included its reactance in X_g, transformer is modeled as ideal LTC. Considerable amount of capacitor at secondary bus reflects reality.

If load is directly connected to secondary bus, load is modeled as static load Ps + jQs.

If load branch Xt from secondary bus to load bus is modeled, induction motor, constant impedance load, RE, and capacitor are located at load bus. Assumed that shunt reactive loss is compensated by capacitor, only series reactive loss by restraint reactance is considered, and power factor assumed as $Q_m/P_m = 0.1$. Power factor of constant impedance load is assumed as also $Q_z/P_z = 0.1$. Power factor of RE is assumed as $P_p/Q_p = -0.2$, which reflect constant leading power factor operation recently adopted in PV (PhotoVoltaic generation).

In Japan reactance of load branch is in average 0.175 p.u.[(4)], whose considerable part is derived from reactance of distribution transformer. Middle voltage in Japan is 6.6kV, which is rather lower 22kV class that is used in most countries. Also short circuit current is limited as low value as 12.5kA. These were effective for safety, but short circuit capacity of distribution network is limited as $\sqrt{3}$ * 6.6kV * 12.5kA = 143MVA, and voltage egulation of distribution network is spoiled. To realize the small short circuit capacity by distribution transformer, its reactance of 20MVA transformer ,which is generally used in Japan, must be such a high value as 20MVA/143MVA = 0.14p.u. or more, which is much higher than common 77kV class transformers. Thus, load branch must be considered most in Japan, where its reactance is extraordinary high.

Besides, peak demand of example substation is 0.326GW, load branch reactance is 0.5578p.u. * 0.326GW = 0.182p.u. (at peak load base), which is slightly higher than average value.

Fault is modeled as one circuit trip on double circuit transmission line feeding the substation, and realized as increase of X_g (from 0.8132 to 1.318).

Analysis on load directly connected to secondary bus

The analysis method does not reflect real structure, but generally used in practice.

P-V curve　P-V curves when transmission line is two circuits and one circuit, and power-voltage characters of constant impedance load (CZL) and constant current load (CIL) are shown in 4.2. Initial power flow is selected as 0.50GW, which is the maximum value appearing in the analysis of example system. A is initial condition. When line turns to one circuit, equilibrium shifts to B by CZL or to C by CIL. Equilibriums in one circuit cases are stable, therefore, voltage collapse never occurs in the system.

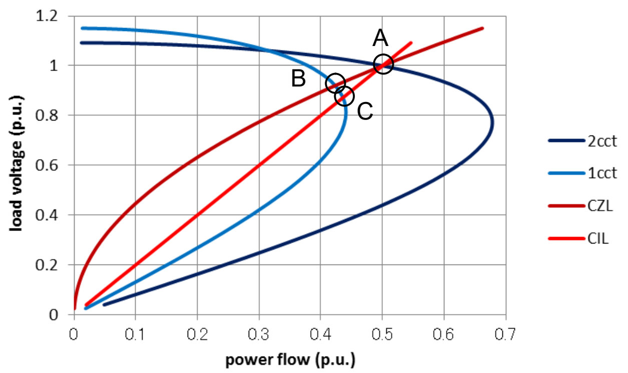

Fig. 4.2　P-V curves and load's power voltage characters

When initial power flow is 0.50GW, one circuit P-V curves by different tap N are drawn as Fig. 4.2. Region nearby equilibrium with power load character of CZL is enlarged. N is 1.2 or less, load voltage rises by tap rise, but drops by tap rise at Nis 1.3 or more and load voltage cannot reach initial voltage 1. Thus it is possible to moving of

LTC by P-V curves, but figure is quite complicated, and many figures are needed for identifying voltage stability limit. That is quite inconvenient.

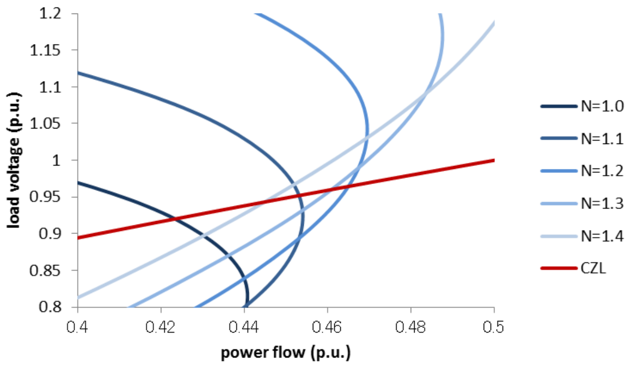

Fig. 4.3 P-V curve by tap position

N-V curve Therefore, another analysis method for LTC, here is proposed N-V curve, which draws secondary voltage V2 by varying tap N. When tap is N, system side seen from secondary bus is expressed as voltage source N Vg behing reactance N^2 Xg.

N-V curve varies by Initial down power flow (that is load amount here). Modeling $Ps \propto V2^{1.2}$, $Qs \propto V2^2$ load, N-V curves are drawn by initial power flow as Fig. 4.4. If peak value of V2: V2max exceeds initial voltage 1, secondary voltage can recover to 1.

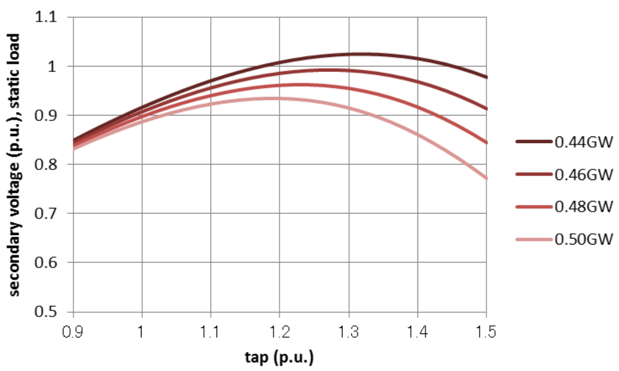

Fig. 4.4 N-V curve by initial power flow (static load)

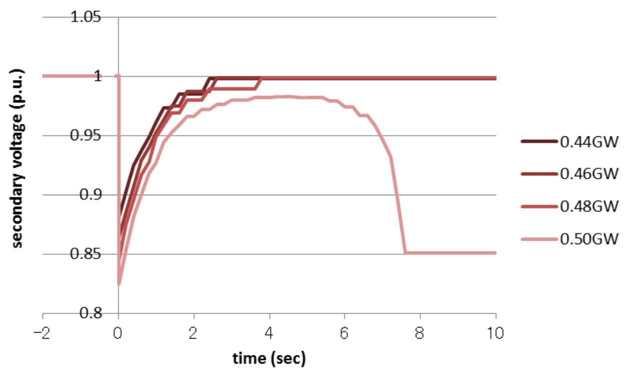

Fig. 4.5 Long term voltage simulation (static load)

As simulation corresponding to N-V curve, long term voltage calculation program (V method) is available. The result is shown in Fig. 5. Voltage sensitivity of load's active power's is modeled as $Ps \propto V^{1.2}$, because in some cases calculation stopped due to ill conversion when modeled as $Ps \propto V^{1.0}$ as usual.

While the system was stable with 0.44GW initial flow or less, is stable at 0.48GW or less flow in simulation, which shows slightly better voltage stability than analysis. The reason is thought that simulation is dispersed calculation and has dead band, and analysis is continuous calculation and does not have dead band.

In N-V curve, induction motor load cannot be modeled, but can be approximately considered. In case of induction motor whose shunt reactive loss is compensated by capacitor, active power is almost $Pm \propto V_2^0$, therefore, its current is almost $Im \propto V_2^{-1}$, and series reactive loss is almost $Qm \propto V_2^{-2}$. Constant impedance (CZ) load's voltage sensitivity is $Pz \propto V_2^1$ and $Qz \propto V_2^2$. Therefore, mixed load of 50% motor and 50% CZ will show voltage sensitivity of $P_L \propto V_2^1$ and $Q_L \propto V_2^0$. Real character will turn away from those just after disturbance or during very low voltage. However, these modeling is possible in quasi-static state. Analysis result is shown in Fig. 4.6. Curve form is quite different from static load case and ill conversion appears in large N.

N-V curve can also consider RE. To static load with $Ps \propto V_2^1$ and $Qs \propto V_2^1$ voltage sensitivity, RE with voltage sensitivity of $Pp \propto V_2^1$ and $Qp \propto V_2^1$ is added and assumed to operate at 0.2GW – j0.04GVar. Analysis result is shown in Fig. 4.7. Curve form is like static load case.

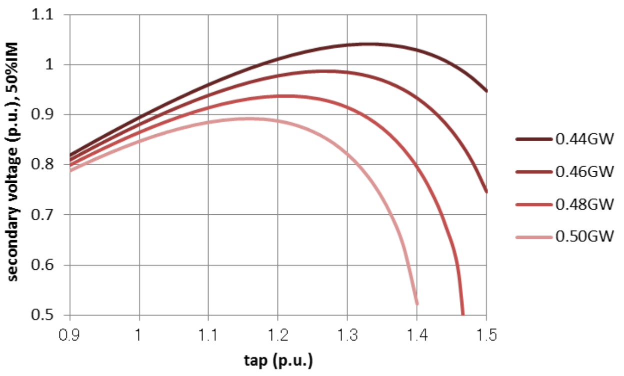

Fig. 4.6 N-V curve by initial power flow (IM load)

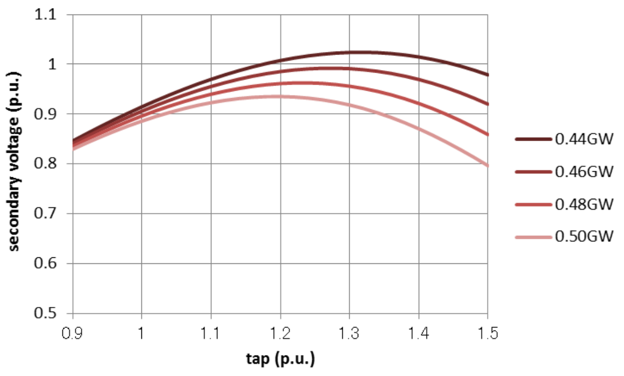

Fig. 4.7 N-V curve by initial power flow (static load + RE)

To identify the initial power flow at voltage stability limit, pairs of initial power flow value and V2max – 1 value are plotted as Fig. 4.8. Four pairs is approximated by parabolic curve, and initial power flow that gives V2max – 1 = 0 is identified. As the results, all of static load, induction motor load, and static load with RE cases give the same voltage stability limit, 0.455GW. If initial flow is less than the limit, secondary voltage can recover to initial value.

Voltage stability limit of the three cases by N-V curve analysis is summed up in Fig. 4.9 by initial power flow and initial load amount.

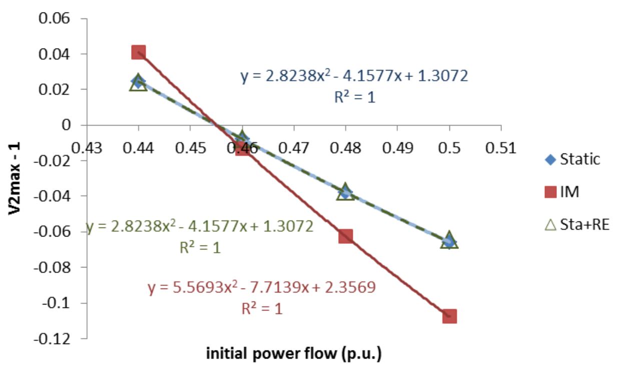

Fig. 4.8 V2max-1 value by initial power flow

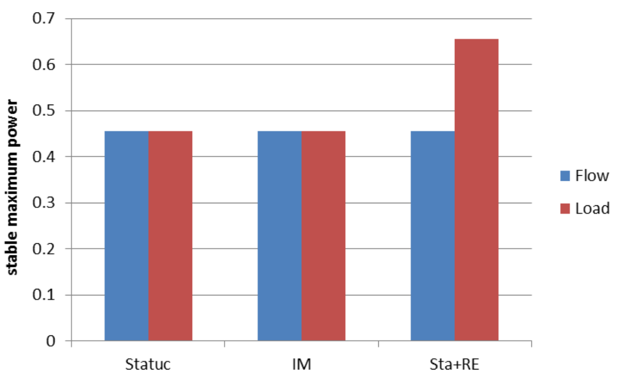

Fig. 4.9 Voltage stability limit initial flow/load

Existing LTC tap range is around 0.9 to 1.1, and such extreme ratio 1.5 is not seen. Even joining distribution transformer’s LTC, tap ratio will be at most around 1.2 or a little more. In reality, secondary voltage is kept constant when LTC reaches its ceiling. Then even if secondary voltage cannot recover to 1, and certainly that is not favorable, the phenomenon is not “voltage collapse” in which voltage become to 50% or lower.

In the figure, stability limit initial flow takes the same value. Stability limit initial load is larger by 0.2GW in only 0.2GW RE output case.

It is a matter of course that these results are conducted. Because in N-V analysis, active and reactive power of any loads and any REs take the same values of initial condition, only if secondary voltage can recover to initial value. Thus, voltage stability limit only depends on initial power flow, and never depends on character of load and RE. Voltage stability limit load will increase by RE output.

However, are these true?

Analysis considering load branch It is already reported in Ref. (2) that modeling of load branch is indispensable to reproduce load’s behavior in voltage sag well by simulation. The same opinion is seen in US(5). If so, modeling of load branch will be also indispensable in one circuit trip case.

T-ω curve In N-V curve analysis without modeling load branch, voltage collapse never appeared, within initial power flow 0.50GW or less and realistic tap range, even though secondary voltage cannot recover to initial value. In addition, tap change is slow. Therefore, much faster induction motor's stall phenomenon is focused. For analysis T-ω curve introduced Ref. (1) is available.

For initial value calculation, circulation is needed. First, some load voltage Vt is assumed. Then, motor's active and reactive power is calculated as follows.

$$\mathrm{Pm} = \frac{\mathrm{Vt}^2\,\mathrm{Rm}}{\mathrm{Rm}^2 + \mathrm{Xm}^2}\ , \quad \mathrm{Qm} = \frac{\mathrm{Vt}^2\,\mathrm{Xm}}{\mathrm{Rm}^2 + \mathrm{Xm}^2} \qquad (4.1)$$

Into the result adding constant impedance load Pz + jQz and removing RE output Pp + jQp, residual load power Pt + jQt is obtained.

Assuming that load bus angle is lagging by δ than secondary bus, residual load power is calculated as follows.

$$\mathrm{P_t} = \frac{\mathrm{V2\ Vt}\sin\delta}{\mathrm{Xt}}\ , \quad \mathrm{Qt} = \frac{\mathrm{V2\ Vt}\cos\delta - \mathrm{Vt}^2}{\mathrm{Xt}} \qquad (4.2)$$

Erasing δ, equation as follows is conducted. と表わされる。これから位相角□を消去すると方程式

$$\mathrm{Vt}^4 + \{2\mathrm{Xt\ Qt} - \mathrm{V_2}^2\}\ \mathrm{Vt}^2 + \mathrm{Xt}^2\,(\mathrm{Pt}^2 + \mathrm{Qt}^2) \qquad (4.3)$$

Solving the equation, Vt is obtained. The Vt value is substituted into eq (4.1). Theses process is repeated until error becomes sufficiently small.

Thus load bus initial voltage Vt and motor's secondary resistance Rm is obtained. Simultaneously initial admittance of CZ load Gz + jBz and hat of RE Gp + jBp are obtained as follows.

$$\mathrm{Gz} + \mathrm{jBz} = \frac{\mathrm{Pz} - \mathrm{jQz}}{\mathrm{Vt}^2}\ , \quad \mathrm{P_p} + \mathrm{jB_p} = \frac{-\,\mathrm{Pp} + \mathrm{jQp}}{\mathrm{Vt}^2} \qquad (4.4)$$

Motor's secondary resistance Rm at speed ω is generally calculated as follows.

$$\mathrm{R2} = \mathrm{Rm}\,(1 - \omega) = \mathrm{Rm_0}\,(1 - \omega_0) \qquad (4.5)$$

Here, R2 is secondary winding resistance (at ω = 0) , $\mathrm{Rm_0}$ and ω_0 are secondary resistance and speed at standard condition. Load voltage Vt is calculated using initial admittance. By the Vt motor's secondary resistance and nonlinear RE admittance vary. Thus repeated until error becomes sufficiently small. Thus T-w curve is obtained.

T-ω curve without RE is shown in Fig. 4.10. in accelerating torque Ta = Te – Tm, that is, excessive torque of electric torque Te over mechanical torque Tm

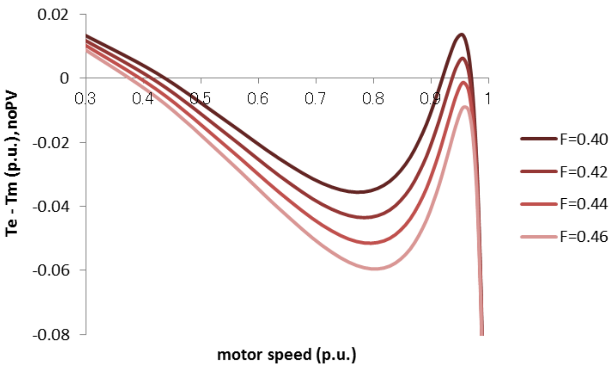

Fig. 4.10 Acceleration torque by initial power flow (w/o RE)

is shown. Mechanical torque is assumed as proportional to squared speed ω^2. The curve varies by initial power flow. The load is stable in 0.42GW flow or less, and unstable in 0.44GW flow or more.

Simulation result of the same case is shown in Fig. 4.11. The load is stable in 0.42GW flow or less, and unstable in 0.44GW flow or more. The result well agrees with T-ω curve analysis.

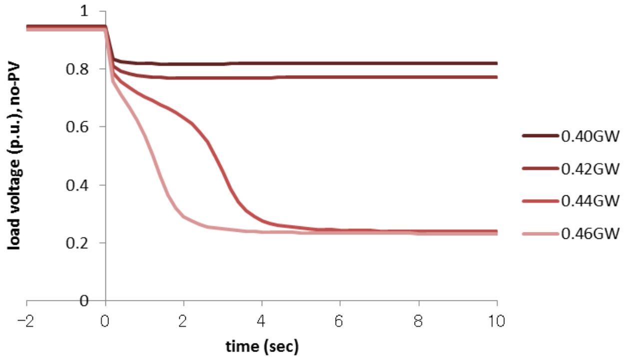

Fig. 4.11　RMS value simulation (w/o RE)

Here assumed that constant impedance RE generates 0.2GW-j0.4GVar. Power factor of RE is slight leading as Qp/Pp = -0.2. T-w curve is shown in Fig. 4.12. In the figure, acceleration torque Ta = Te – Tm, that is, excessive torque of electric torque Te over mechanical torque Tm is shown. T-ω curve varies by initial power flow. The system is stable in 0.30GW flow or less, and unstable in 0.32GW flow or ore.

T-w curve with constant current RE generating 0.2GW-j0.4GVar is shown in Fig. 4.13. In the figure, acceleration torque Ta = Te – Tm, that is, excessive torque of electric torque Te over mechanical torque Tm is shown. T-ω curve varies by flow. The system is stable in 0.36GW flow or less, and is unstable in 0.38GW flow or more.

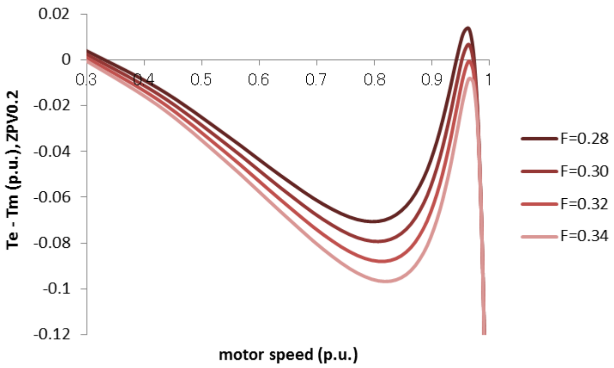

Fig, 4.12　T-ω curve by initial flow (with 0.2 CZ-RE)

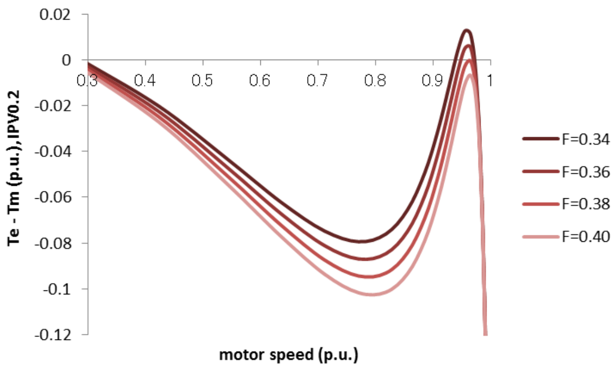

Fig. 4.13　T-ω curve by initial flow (with 0.2 CI-RE)

To identify stability limit, peak value of accelerating torque at high speed region by initial flow are plotted as Fig.4.14. Four plots are approximated by parabolic curve, and the initial flow making the peak value as zero. Stability limit varies by load and RE. Stability limit is expressed by initial flow and load amount as Fig. 4.15.

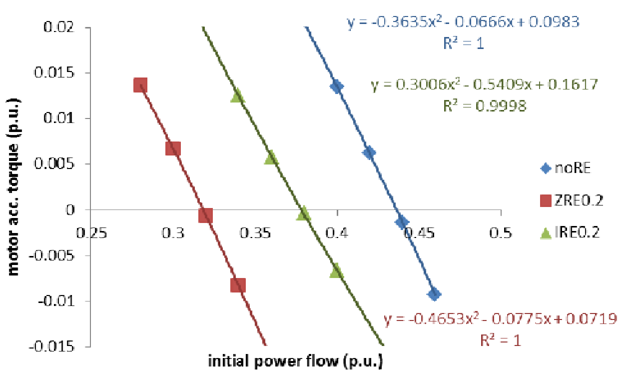

Fig. 4.14　Acceleration torque by initial flow

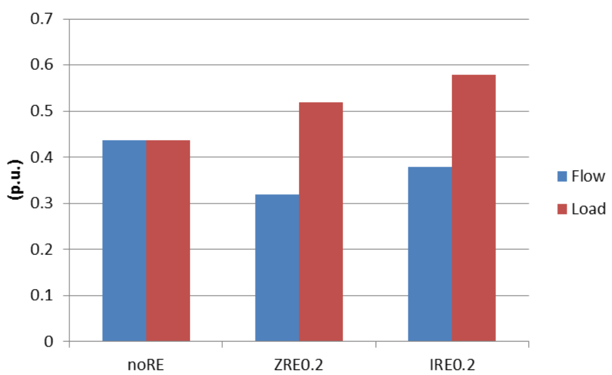

Fig. 4.15　Stability limit flow/load by RE design

Voltage stability limit when RE output is 0.2GW certainly exceeds that when RE is not interconnected in load amount, however, does not reaches in initial power flow. Therefore, voltage stability cannot be managed by load flow, but RE output must be known. Besides, stability limit is considerably extended by constant current RE compared to constant impedance RE.

To study the reason, CZ load power Pz, RE output Pp, motor's electric torque Te and mechanical torque Tm, and load voltage Vt in cases of constant impedance RE (ZRE) and constant current RE (IRE) are compared in Fig. 4.16. For convenience of graduation, half of load voltage is shown.

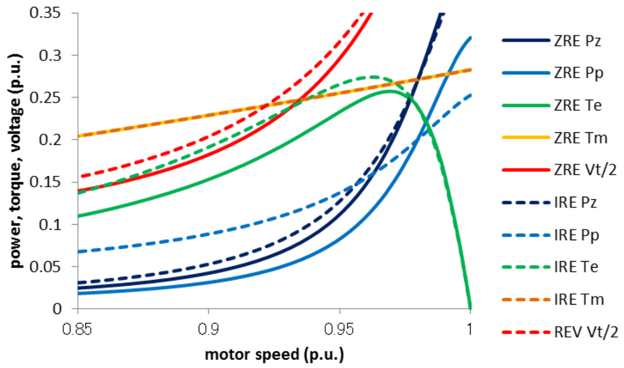

Fig. 4.16 T-ω and P-ω curves by RE design

When motor decelerates load voltage drops. During low voltage, IRE output exceeds ZRE output. Some part of the excess is divided to CZ load, but considerable part contributes motor's electric torque Te. As the result, Te is lower than mechanical torque Tm in all speed range in case of ZRE, but Te exceeds Tm in some speed range in case of IRE, thus motor is kept stable.

Voltage unstable accompanied with voltage sag

Up to here one circuit trip on double circuit line, here one circuit is assumed to trip due to three-phase-to-ground fault. By the fault voltage drops to almost zero. Then, induction motor cannot receive power from system. On the contrary mechanical load consumes power. Motor solves the mismatch by dispensing its rotating energy. For example, when 50% mechanical load of capacity, 0.5 sec inertia, 100% sag depth during 0.1 sec are assumed, motor decelerates during voltage sag around

$$0.1\text{sec} / (0.5\text{sec}/50\%) = 10\%$$

If speed before sag is 0.977, speed after fault clear is 0.877. Deceleration by voltage sag makes load's stability worse. It is a matter of course that some fault is accompanies with one circuit trip, so practical stability limit load amount becomes smaller than without fault case.

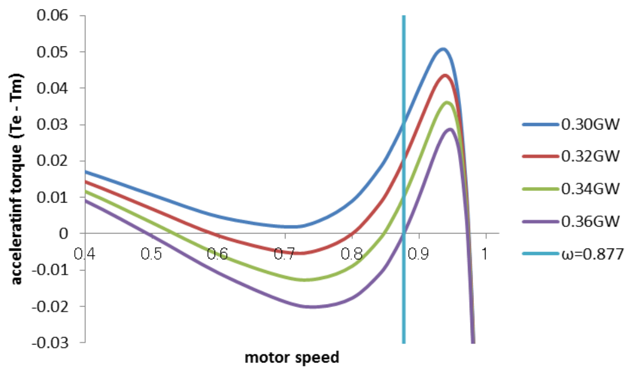

Fig. 4.17 T-ω curve when one circuit trip (with LB)

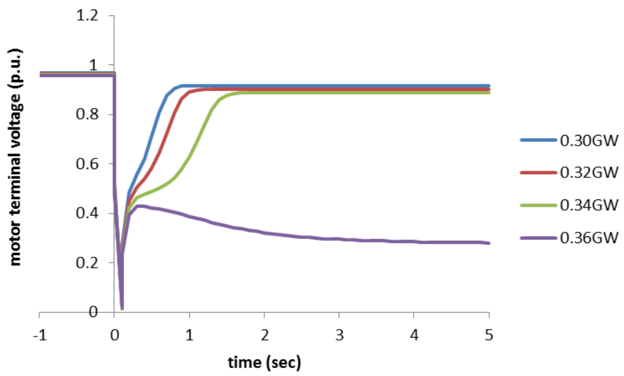

Fig. 4.18 One circuit trip simulation (IM load, with, LB)

At first, T-ω curve in case of induction motor load and load branch (LB) is modeled. Assuming speed at fault clear is 0.877, motor can recovered to proper operation if accelerating torque at the speed is positive. If negative, motor goes to stall. The result is shown in Fig. 4.17. When load is 0.34GW or less, accelerating torque at 0.877 speed is positive, therefore, is stable. When load is 0.36GW or more, accelerating torque at 0.877 speed is slightly negative, therefore, is unstable. By motor deceleration during sag, stability limit load amount becomes smaller than case without voltage sag.

In the same case RMS simulation is held. The result is shown in Fig. 4.18. When load is 0.34GW or less, motor voltage recovers to normal, but when load is 0.36GW, notor voltage still remain at very low (stall). Stability limit load amount is well agree with T-ω curve analysis.

Difference in stability by power system model Different power system model gives different analysis result. Power system models of 2*2 = 4 cases as follows are considered.

Load: induction motor load / static load model aggregation: LB is modeled / LB is ignore

Simulation result of IM load and LB modeled case is already shown in Fig. 4.18. Simulation results in the other three cases are shown in Fig. 4.19 to 4.21.

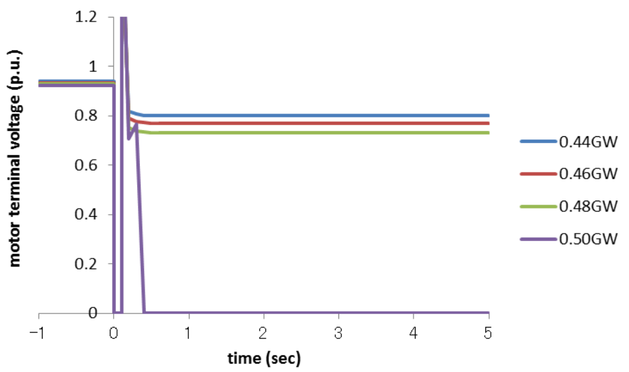

Fig. 4.19 Simulation of one circuit fault (static L, with LB)

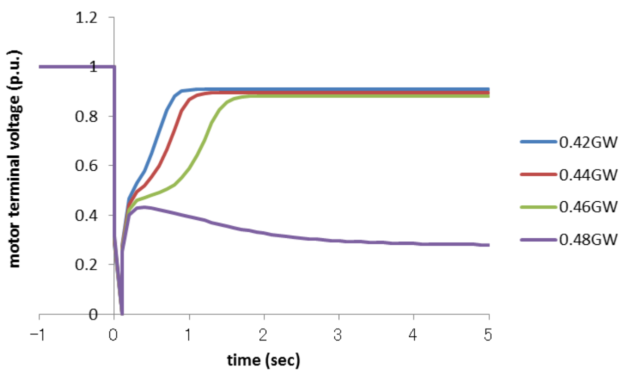

Fig. 4.20 Simulation of one circuit fault (IM L, w/o LB)

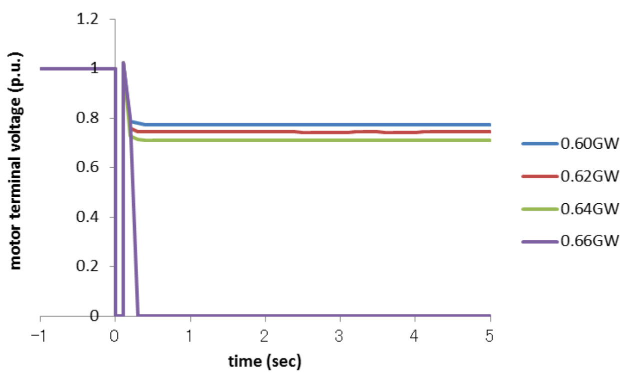

Fig. 4.21 Simulation of one circuit fault (static L, w/o LB)

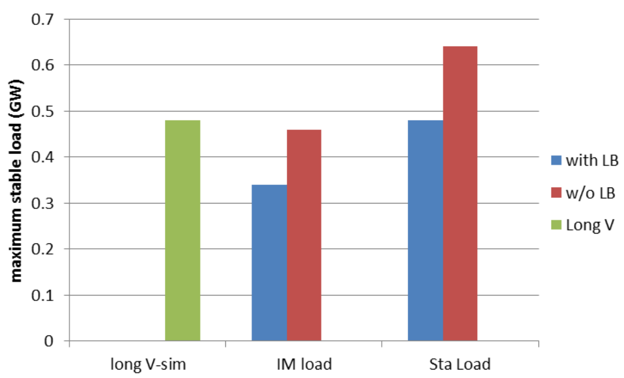

Fig. 4.22 Voltage stability limit by system model

In case of static load and modeling LB case shown in Fig. 4.19, stability limit load amount becomes as large as 0.48GW. Also in case of IM load and ignoring LB case shown in Fig. 4.20, stability limit is as large as 0.46GW. Moreover, in case of static load and ignoring LB case, stability limit is as large as 0.64GW, which is larger than stability limit of tap operation (0.48GW, Fig. 4.5). Of course, only IM load and modeling LB case is true and the others are false. However, it must be noticed that the false three cases show very large and optimistic stability limit.

Results above are compared as Fig. 4.22, including long term voltage simulation without grounding fault as reference. By either employing static load model or ignoring load branch, voltage stability is assessed as the same or better as long term voltage simulation without modeling ground fault. Only IM load and modeling LB case shows smaller stability limit.

Since IM load model is not used for power system analysis in Japan, it is wrongly believed that main factor deciding voltage stability limit is tap operation even if grounding fault is considered, and that nothing but long term voltage simulation is the measure for assessing voltage stability limit. Here, importance of realistic power system model is demonstrated.

Effect of partial load drop

Power system can be faithfully reflecting reality by employing induction motor load and load branch. Besides, according to study in chapter 2, 30% of load stops due to sufficiently deep voltage sag. What stops is not motor load. By the partial load stop, possibility of motor stall is reduced.

Assuming that 60% of not motor load (30% of total load because motor ratio is 50%) stops, T-ω curve is drawn as Fig. 4.23. Assuming that motor speed is reduced to 0.877, accelerating torque is positive at the speed, therefore stable, when load amount is 0.40GW or less, however, accelerating torque turns negative at the speed, therefore unstable, when load amount is o.42GW or more. Load amount at stability limit increases considerably by partial load drop.

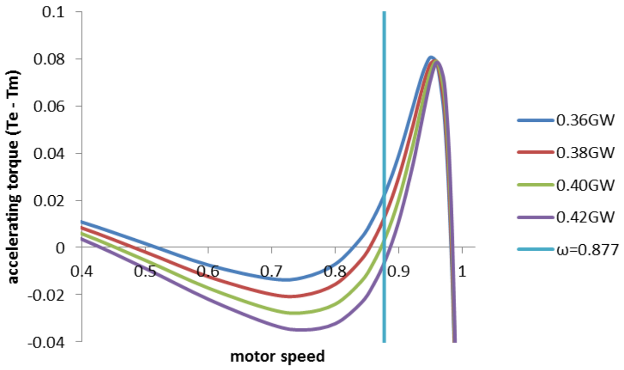

Fig. 4.23 T-ω curves with partial load drop

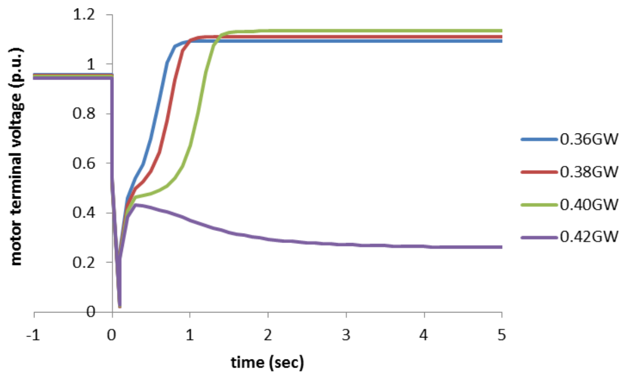

Fig. 4.24 RMS simulation with partial load drop

RMS simulation result is shown in Fig. 4.24. When load amount is 0.40GW or less, load voltage recovers to normal. When load amount is 0.42GW, motor goes to stall. RMA simulation result well agrees with T-w curve analysis result.

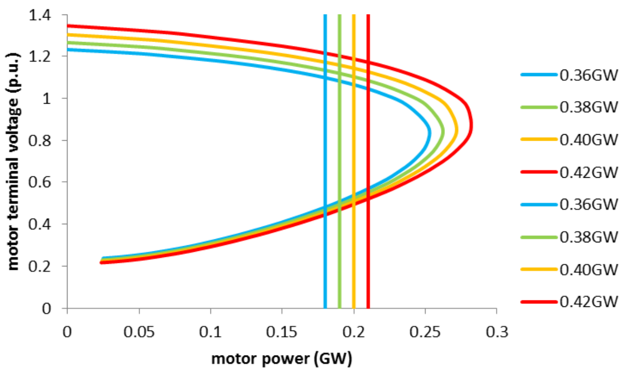

Fig. 4.25 P-V curve with partial load drop

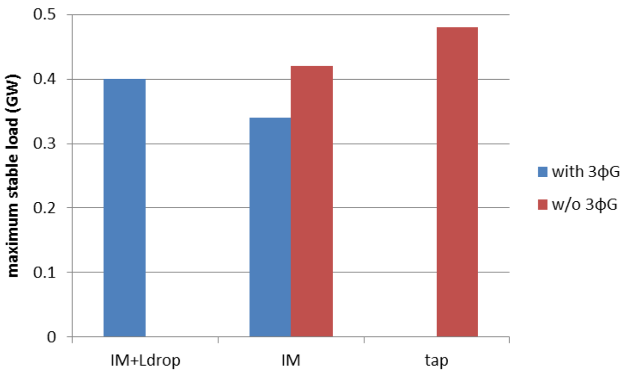

Fig. 4.26 Summing up voltage stability of the local system

The phenomenon is solved by P-V curve as Fig. 4.25, where all cases are judged as stable. This is clearly different from reality. The reason is that P-V curve can handle neither deceleration of motor due to voltage sag, nor judging whether the motor recovers to normal. Although P-V curve is the most popular analysis method for voltage stability in Japan, it must be noticed that every question around voltage stability is not necessarily solved by P-V curve.

Voltage stability of a pure load local system is studied from various points of view. Four load amounts of voltage stability limit from different point of view are compared. Limit of slow voltage collapse was 0.48GW. Limit of fast voltage collapse without voltage sag was reduced to 0.42GW. That with voltage sag was greatly reduced to 0.34GW. Impact of 10% motor deceleration was quite large. There considering partial 30% load drop due to sag, limit increased to 0.40GW. This, stability limit varies by power system model and analysis method. Importance of selecting power system model and analysis method will be recognized.

Voltage stability by RE design[1][6]

By the study above, impact by highly integrated RE on power system voltage stability can be assessed. As RE design, those three as follows are assumed.

“Drop” type RE stops due to voltage sag. Voltage collapse may occur until it comes back.

“FRT” type RE does not stop due to voltage sag, but does not support voltage recovery after sag.

“DVS” type RE does not stop due to sag, and supports voltage recovery after sag.

FRT is abbreviation of “Fault Ride-Through”, and DVS is that of “Dynamic Voltage Support”. Dynamic character of DVS RE is expressed as follows here.

$$G_{RE} = G_{RE0},$$
$$B_{RE} = Y_{RE0}\ \{(V_C / V_{C0})^2 - (V_C / V_{C0})^{2+K}\}$$

Active power is assumed as constant conductance G_{RE}. Of course constant current and constant power controls are possible. However, it is unreasonable to complete constant power control during voltage sag due to network fault. On the contrary, constant conductance control has no unreasonable items.

Reactive power is expressed as susceptiance varying by voltage. Y_{RE0} is admittance at rated power output. The character is shown in Fig. 4.27. FRT type corresponds to K = 0 case, where reactive power is zero in all voltage range. DVS type of K takes 2 or larger, and larger K means powerful voltage support. Here K is chosen as 5 to 10 so that excessive reactive power variation would not generated by very small voltage disturbance.

To say the truth, This DVS does not fully use inverter’s current capacity. Design that use capacity thoroughly is of course possible, however, here demonstrated that even these light DVS can present dramatic effect on voltage stability improvement.

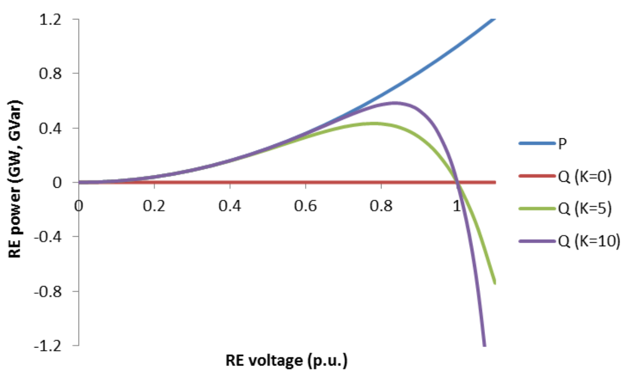

Fig. 4.27 Power-voltage character of DVS type RE

RE is parallel connected to load bus, because the location is most effective foe reducing network equipment. RE output is assumed as 20% of load power. Load is assumed as mixture of 50% induction motor and 50% constant impedance. Fault is modeled one circuit 3LG-O on double circuit transmission line with 0.1 sec Fault clear time. 30% load is assumed to stop due to voltage sag. No

RE case is already shown in Fig. 4.23 and 4.24.

In case of drop type RE whose output is 20% of load considering partial load drop, T-ω curve is shown in Fig. 4.28. Simulation result is shown in Fig. 4.29. Load amount 0.38GW or less is stable, and 0.40GW is unstable.

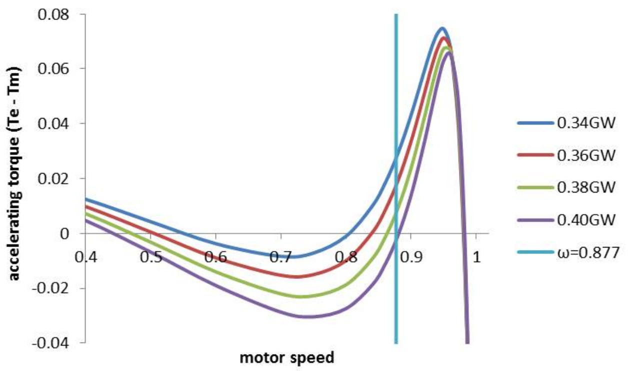

Fig. 4.28　T-ω curve (drop RE, with load drop)

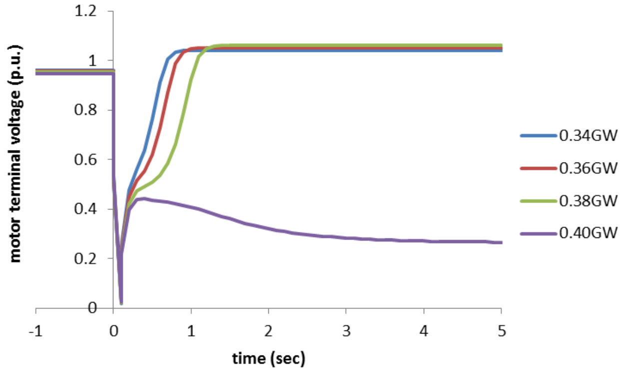

図 4.29　RMS simulation (drop RE, with load drop)

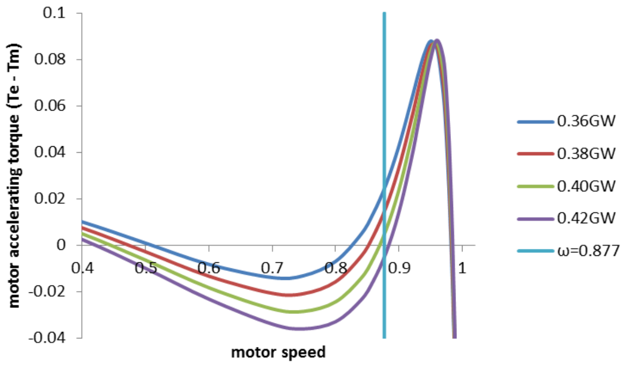

Fig. 4.30　T-ω curve (FRT RE, with load drop)

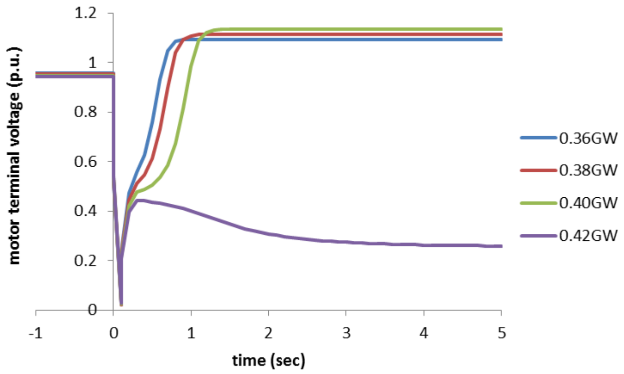

Fig. 4.31　RMS simulation (FRT RE, with load drop)

In case of FRT type RE whose output is 20% of load considering partial load drop, T-ω curve is shown in Fig. 4.30. Simulation result is shown in Fig. 4.31. Load amount 0.40GW or less is stable, and 0.42GW is unstable.

In case of DVS type RE whose output is 20% of load considering partial load drop, T-ω curve is shown in Fig. 4.32. Simulation result is shown in Fig. 4.33. Load amount 0.44GW or less is stable, and 0.48GW is unstable. 0.46GW case is judged as unstable by T-ω curve, but as stable by simulation. The error seems to appear due to repeated calculation accuracy in T-ω curve.

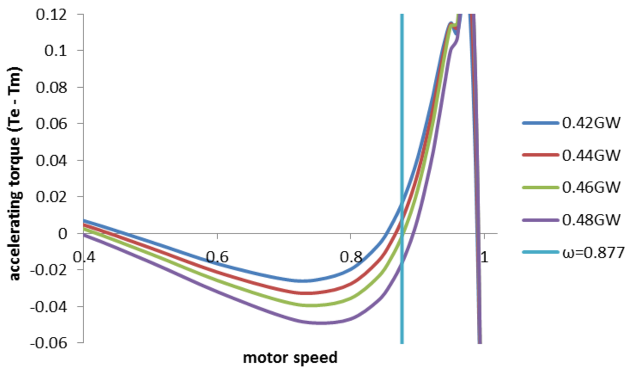

Fig. 4.32　T-ω curve (DVS RE, with load drop)

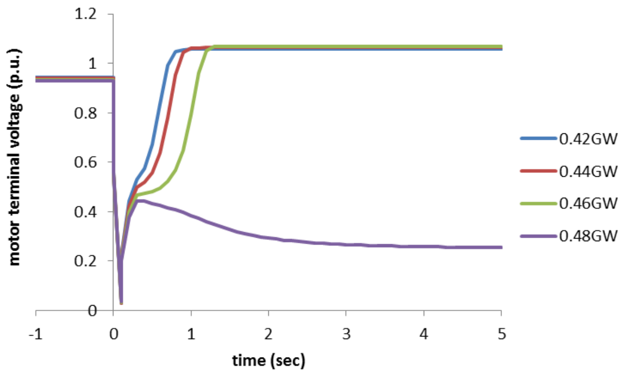

Fig. 4.33　RMS simulation (DVS RE, with load drop)

Voltage stability limit is assessed by initial load, initial flow and flow after fault as Fig. 4.34. Limit of DVS type seems to be splendidly larger than limit of no RE in viewpoint of initial load. However, it must be noticed that limit of DVS type cannot reach the limit of no RE in viewpoints of initial flow and flow after failure. The result tells that network equipment's reduction by RE cannot be evaluated by full-mark even if RE is DVS type. The reason is that induction motor load amounting 50% of load spoils voltage stability very much. Also importance of modeling induction motor load and load branch must be understood.

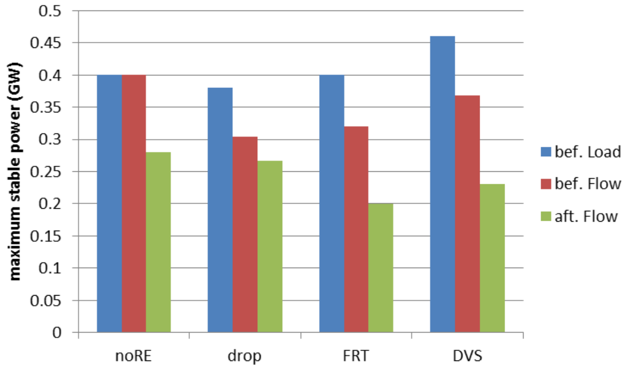

図 4.34　RE の設計による安定限界の違い

Analysis examples of Trunk System

Above, local system such as a pure load primary substation fed by 154kV double circuit line is studied. The reason is that the simple example is favorable for understanding voltage stability issues. Analysis is so easy that readers can examine. It must be understand that the truth is not known surprisingly. However, real target is voltage stability of trunk system. It has become noticed that stability problems exist here and there in trunk system if system is modeled reflecting the reality. Since the all cannot describe in limited space, two examples are introduced here.

Example of a small trunk system Structure of the system is shown in Fig. 4.35. Large power is received via three interconnection. Right side interconnection is assumed to be lost by three-phase failure with 0.07 sec clearing time. Load is mixture of 50% motor and 50% impedance. Partial load drop due to sag is considered, but without load drop case is also studied as reference. Load drop ratio is decided by sag depth of each load. The part with light gray background is a considerable sized radial system after the fault, is affected by deep voltage sag because the fault occurs on interconnection to outer system. Fast voltage collapse becomes serious. Simulation results in LB omitted, LB modeled, LB modeled and LB and load drop modeled cases are shown in Fig. 4.36 to 4.38.

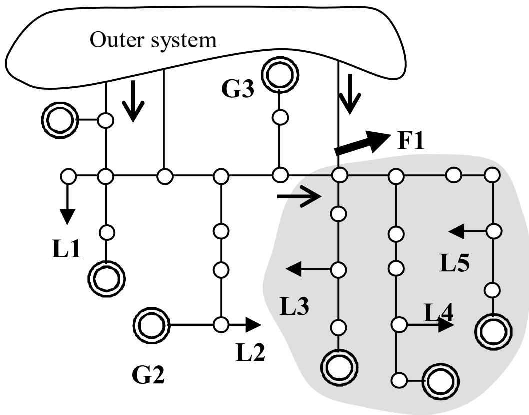

Fig. 4.35　Structure of small trunk system

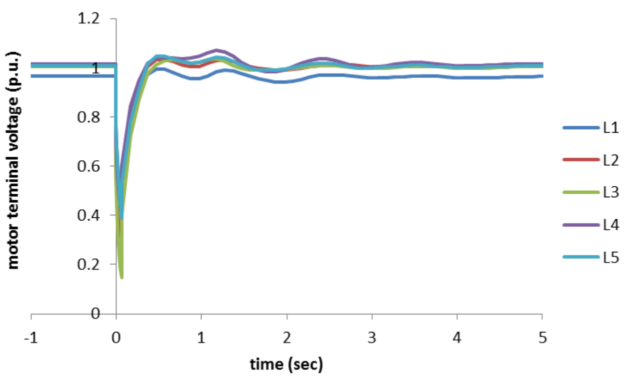

Fig. 4.36　RMS simulation (w/oLB, no RE)

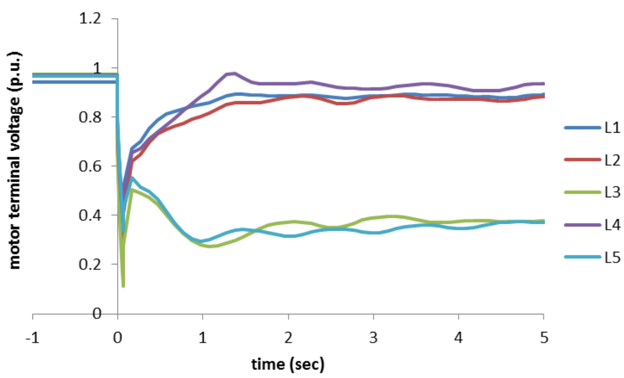

Fig. 4.37　RMS simulation (with LB, no RE)

In case of LB omitted and without load drop, voltage recovery is very fast in all loads. In case of LB modeled and without load drop, load L3 and L5 fall in voltage collapse. In case of LB modeled and with load drop, voltage recovers in all loads but the recovered voltage goes higher because of reactive loss reduction. Thus, load model significantly affects on simulation results.

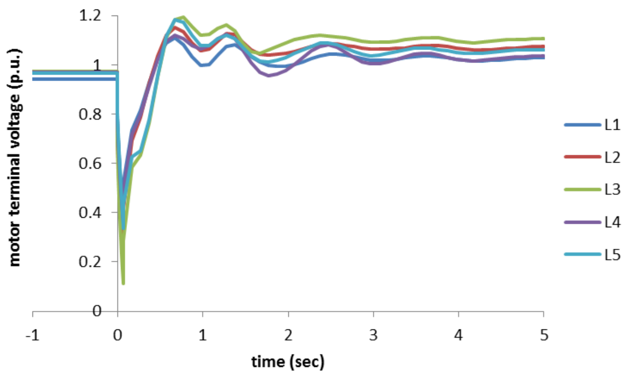

Fig. 4.38 Simulation (with LB & load drop, no RE)

Here the three types of RE with 20% output of load joins. For demand supply balance, some thermal generators stop. LB and partial load drop are modeled. Simulation result in no RE case is already shown in Fig. 4.36. Simulation results of three cases with RE are shown in Fig. 4.39 to 4.41.

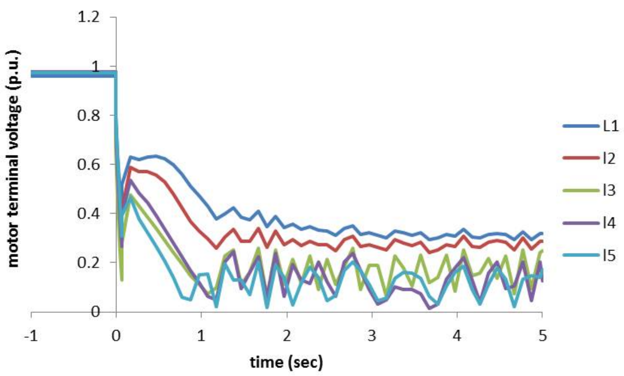

Fig. 4.39 RMS simulation (drop RE)

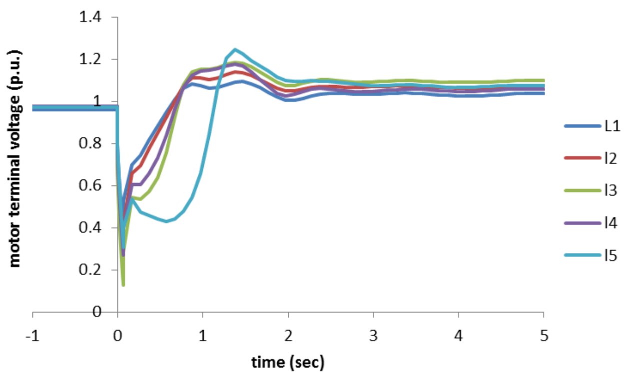

Fig. 4.40 RMS simulation (FRT RE)

In case of drop RE, not only loads L3 to L5 in gray area but also L1 and L2 go to voltage collapse. In case of FRT RE, loads do not go to stall but voltage recovery time is rather long, and voltage considerably rises after fault. In case of DVS type, voltage recovery is fast and voltage rise after fault is mitigated.

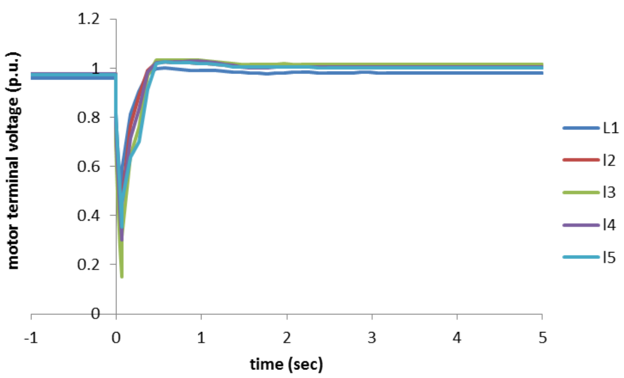

Fig. 4.41 RMS simulation (DVS RE)

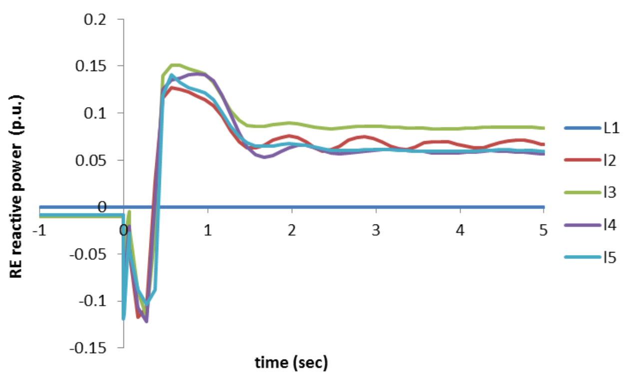

Fig. 4.42 RMS simulation of DVS RE's reactive output

DVS type RE supplies reactive power during low system voltage, and absorbs reactive power and mitigates voltage rise after fault as shown in Fig. 4.42. Certainly REs supplies reactive power until 0.4 sec, and absorbs reactive power after voltage recovery. The operation absorbing reactive power tends to bring overcurrent in inverter, so must not continue long. Practically, automatic voltage control such as capacitor shutdown, reactor joining, tap operation are done and the overcurrent is solved in a short time.

As stated above DVS type RE is special cure for preventing fast voltage collapse. The reason is of course that its voltage-reactive power character is like that of SVC known as voltage stabilizing equipment. In other words, DVS type RE includes SVC function. Since one equipment can perform two function, of course, it is economical. Most RE employs OGBT (Insulated Gate Bipolar Transistor) for interconnecting inverter. IGBT has high possibility such as SVC function. However, its high ability is not sufficiently used now. It is said to be as quite inefficient, and such a situation must be improved.

Example of a large trunk system Structure of the example system is shown in Fig. 4.43. The system interconnects to a relatively small neighboring system via one tie line, but almost forms a large islanded system. One circuit of double circuit line is tripped by three-phase fault as F1. Fault clearing time is 0.07 sec. Load is mixture of 50% motor and 50% impedance. Partial voltage drop is considered, but without load drop case is also studied as reference. Load drop ratio is decided by sag depth at each load.

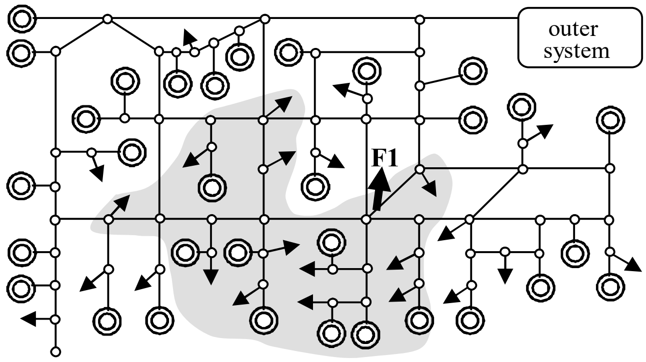

Fig. 4.43 Structure of the large trunk system

Since local generation is poor in area with light gray background, voltage support ability of system, so voltage collapse becomes serious. Relatively light fault as one circuit 3LG-O may bring serious problem, because fault location F1 is an important path through which much power is imported to the gray area with poor voltage stability.

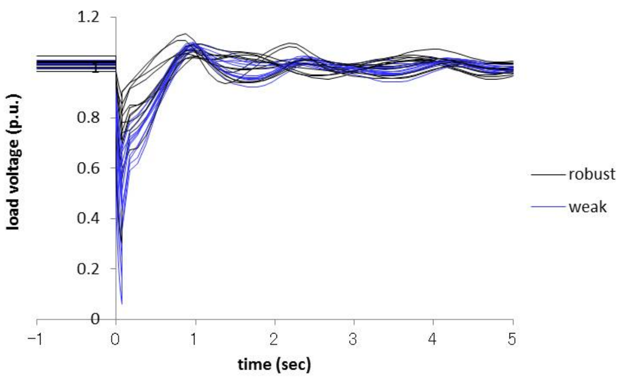

Fig. 4.44 RMS simulation (w/o LB, load drop)

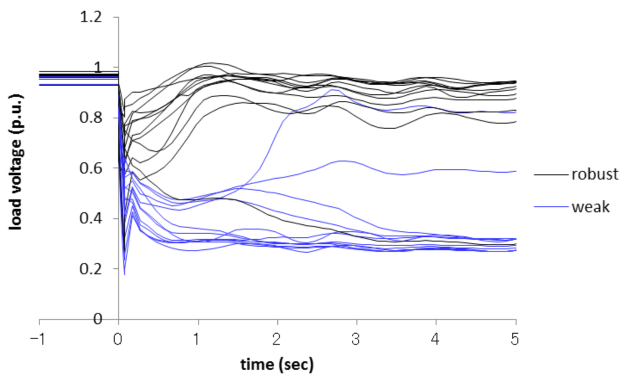

Fig. 4.45 RMS simulation (with LB, w/o load drop)

Simulation results are shown in Fig. 4.44 to 4.46. Loads with poor voltage support in gray area is shown as blue line, and the others are shown as black line.

In case without LB and load drop, voltages of all loads recover as soon as 1 sec. In case with LB and without load drop, almost all loads with poor voltage support go to voltage collapse. In case with LB and load drop, voltages of all load can recover, as long as 2.5 sec is needed for the recovery. Usual permitted low voltage

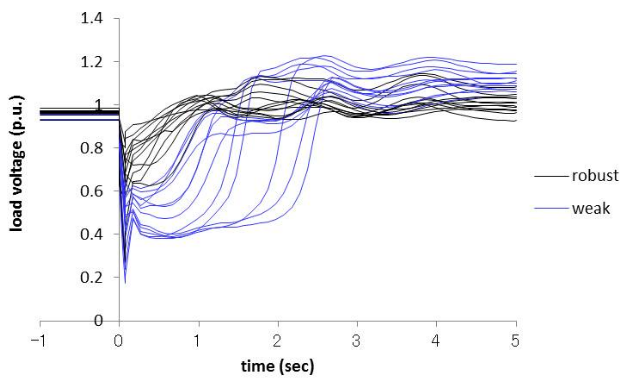

Fig. 4.46 RMS simulation (with LB, load drop)

duration is 1 sec in most equipment such as voltage sag compensator and FRT type inverter. By such a long voltage sag that FRT RE does not anticipate, much amount of RE trips, and of course FRT function is lost. Therefore, trunk system voltage stability becomes threatened.

Three types of RE already introduced is joined with 20% output of load. For demand supply balance, some thermal generator stop. Load branch and partial load drop due to voltage sag is modeled. Simulation result in no RE case is already shown in Fig. 4.46. Three cases with RE are shown in Fig. 4.47 to 4.49.

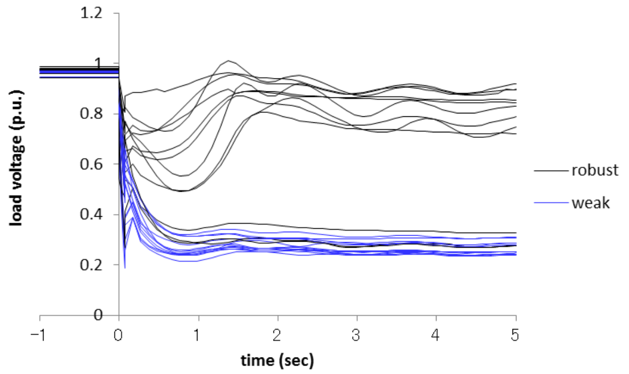

Fig. 4.47 RMS simulation (drop RE, with load drop)

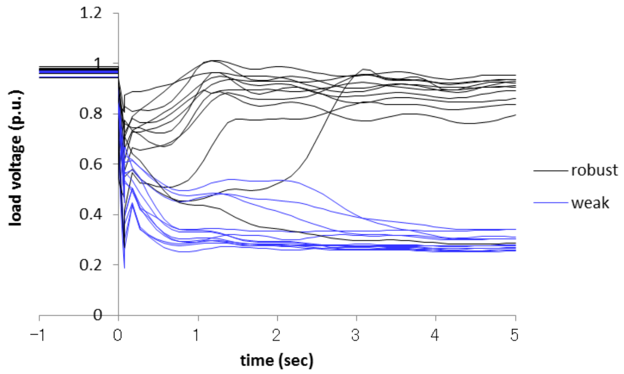

Fig. 4.48 RMS simulation (FRT RE, with load drop)

In drop RE case, not only weakly voltage-supported loads but some robustly voltage–supported loads go to voltage collapse. In case of FRT type RE case, most weakly voltage-supported loads and one load robustly voltage-supported go to voltage collapse. In case of DVS type RE, all loads recover to normal voltage within 1 sec, and shows better stability tan no RE case. Besides, overvoltage after recovery is considerable mitigated.

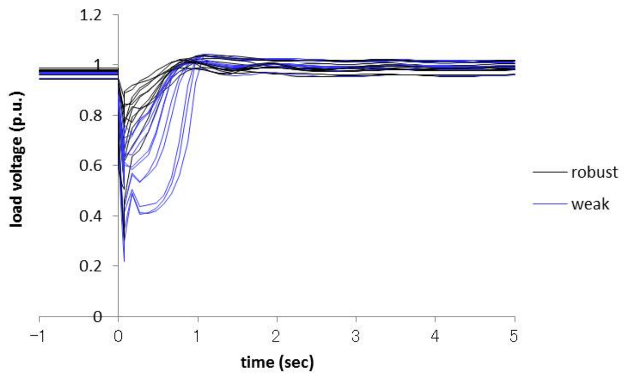

Fig. 4.49 RMS simulation (DVS RE, with load drop)

DVS type RE, as shown in Fig. 4.50, supplies reactive power until voltage recovery and absorbs reactive power after voltage recovery. He voltage absorbing operation tends to overcurrent, so must not continue long. Practically, automatic voltage control such as capacitor shutdown, reactor joining, tap change are performed, and the overcurrent is solved in a short time.

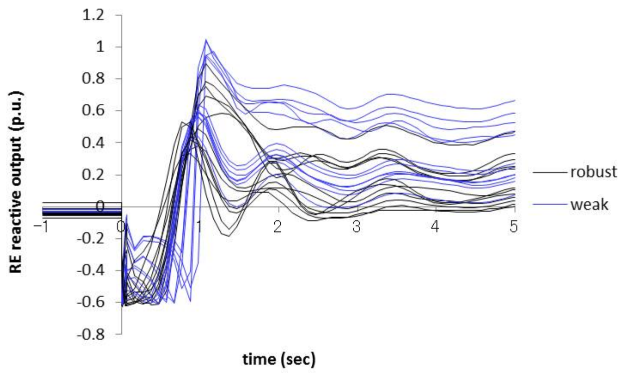

Fig. 4.50 Reactive output of DVS RE

The large trunk system case shows similar tendency as former small trunk system. However the large trunk system has quite poor voltage stability, difference by system model or RE design appear more strongly.

Possibility of voltage collapse Voltage collapse without fault actually occurred in 1987, and can be repeated if reactive reserve is not prepared. Since 20 years, many local thermal generators near load was scrapped, voltage stability becomes generally worse. Possibility of fast voltage collapse accompanied fault is explained in relation with synchronous stability in next chapter.

Method for applying P-V curve for transient voltage stability

On one hand, stall phenomenon of induction motor load could be well explained by T-ω curve considering system side impedance. On the other hand, slow voltage instability by ran away of LTC (on-Load Tap Changer) has been explained by P-V curve. Thus a motive appears to explain also the fast voltage instability (i.e. stall) by P-V curve.

Then, an invention to bring the mechanical torque that is decided not by condition in electric circuit but only by rotating speed into P-V curve. As a typical invention, “stability boundary curve” was recently presented supported by traditional “equal slip line”.

However, in stability boundary curve drawn on P-V plane, suspicious matters are seen. Whether new stability boundary curve is an equivalent theory to established T-ω curve theory or not?

In natural science, if two or more theories exist, usually one survives as truth and the others perish as false. The selection makes natural science more reliable than the other sciences. Here, equivalence of the two theories is examined. As the result, is was verified that they are equivalent. Besides, it is also verified that theories well agree with simulation result.

Theory of T-ω curve　Model used here is shown in Fig. 4.51. Model is always idealized by preserving essential elements on physical phenomenon, and omitting not essential elements. Here, resistance of system side is omitted and reactance Xs only is considered. Motor is expressed by “slip model” where resistance in primary winding and exciting admittance are ignored, as variable internal resistance Rm that is decided only by rotating speed ω (or slip s = 1 - ω) behind constant restraint reactance Xm that is sum of reactance of primary and secondary windings. Rm varies by ω (or s) as follows.

$$Rm = \frac{R_2}{s} = \frac{R_2}{1-\omega} \qquad (4.6)$$

As non-motor load pure conductance Gz and susceptance Bz for maintaining initial load voltage Vr as 1 join in parallel.

Load’s admittance as a whole $\mathbf{Y_L}$ is calculated as follows.

$$\mathbf{Y_L} = Gz + j\,Bz + \frac{1}{Rm + j\,Xm} \qquad (4.7)$$

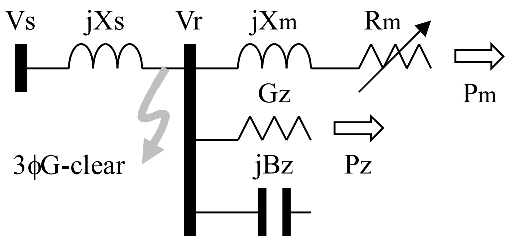

図 4.51　解析に用いたモデル

Load voltage $\mathbf{Vr}$ is calculated as follows.

$$\mathbf{Vr} = Vs \frac{1/\mathbf{Y_L}}{j\,Xs + 1/\mathbf{Y_L}} \qquad (4.8)$$

Motor current magnitude Im is calculated as follows.

$$Im = \frac{Vr}{\sqrt{(Rm^2 + Xm^2)}}$$

Motor consumption power Pm is calculated as follows.

$$Pm = Im^2\,Rm = Im^2\,(R2 + \frac{1-s}{s}\,R2)$$

Here, since motor's shaft output Pm2 is equal to motor consumption power deducted secondary winding loss Im^2 R2 away, is expressed as follows.

$$Pm2 = Im^2\,\frac{1-s}{s}\,R2 = Im^2\,\frac{\omega}{s}\,R2 = \omega\,Im^2\,Rm$$

Besides, motor's electric (input) torque Te is calculated as follows.

$$Te = \frac{Pm2}{\omega} = Im^2\,Rm = Pm = \frac{Rm\,Vr^2}{Rm^2 + Xm^2} \qquad (4.9)$$

That is, motor's electric torque Te is equal to consumption power Pm. The relationship is available only if primary winding resistance is ignored. In general, electric torque is equal to secondary input power.

Motor's mechanical (output) torque Tm is assumed to be proportional to squared speed ω^2. Because it was confirmed by the author in experiment that pump as a main use of motor has the character. Here, Tm0 is initial mechanical torque, ω_0 is initial speed.

$$Tm = Tm0\,(\frac{\omega}{\omega_0})^2 \qquad (4.10)$$

Parameters used in analysis are shown in Table 4.1. They are obtained by aggregating the large system shown in Fig. 4.43into one machine one load.

Motor's rated capacity W_m is assumed as 1.0, and parameters are assumed as follows.

Loading L_m = consumption kW / rated kVA = 0.5

Unit inertia constant M_m = 0.5 sec

These are average values by presumed from load's response in voltage sag.

表 4.1　解析に用いた諸元

Vs	Xs	Vr	Xm	Pm	Rm	ω
1.06	0.725	1.0	0.2	0.5	1.979796	0.975
Gz	Bz	Pz	Wm	Mm	Lm	
0.5	0.363216	0.5	1.0	0.5sec	0.5	

Under these parameters, electric torque Te and mechanical torque Tm are expressed as functions of speed ω as shown in Fig. 4.52. Under these parameters, three equilibriums where electric torque Te is equal to mechanical torque Tm exist. A is stable equilibrium expressing normal operation, B is unstable equilibrium, and C is stable equilibrium expressing stall. When motor decelerates from A by shock of voltage sag beyond B, motor must go to C, stall.

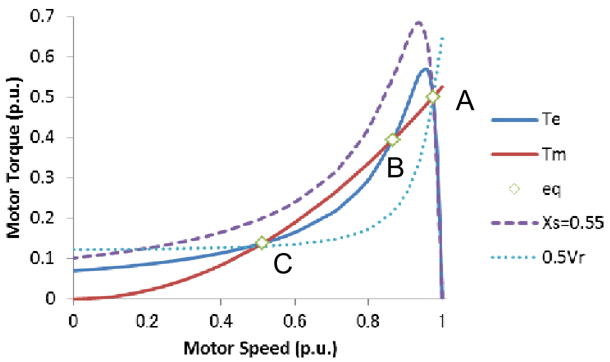

Fig. 4.52　T-ω curve and equilibriums

A case where system condition is easier. Reactance from 66kV bus of primary substation to load is around 17.5% at peak demand base. Deducting the value from original Xs, new Xs value become 0.55. T-w curve in the case is also shown in the figure. B and C disappear. Therefore, stall phenomenon never occurs.

Mapping of T-ω curve onto P-V plane　In the system shown in Fig. 4.51, load voltage Vr is decided when speed ω is decided. Half of Vr (0.5Vr) is also drawn in the figure. Since Vr is an increasing function of ω, horizontal axis of Fig. 4.52 can be changed from ω to Vr. Then, according to tradition that P on horizontal and V on vertical axis are plotted in P-V curve, both axis are changed. Thus, mapping onto P-V plane is obtained.

Since not only motor power but also power of the others are traditionally expressed on P-V plane, adding power of impedance load $Pz = Gz\ Vr^2$ to torque, Te + Pz corresponding electric torque and Tm + Pz corresponding mechanical torque are calculated and Fig. 4.53 is obtained.

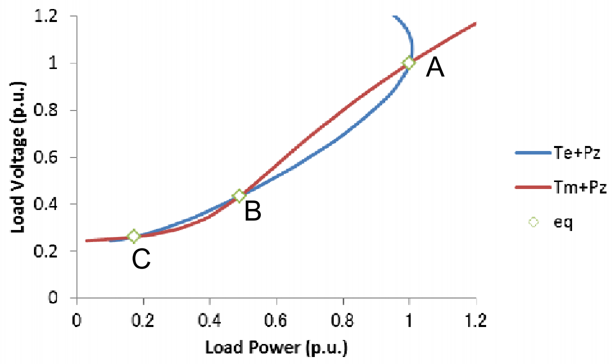

Fig 4.53　Load's P-V curve equivalent to T-ω curve

Te + Pz means supply ability of system side and is usual P-V curve itself. Tm + Pz means power demanded by load and usually used auxiliary. Of course these two lines van be drawn on motor only.

Also on P-V plane, three equilibriums exist where Te + Pz agrees with Tm + Pz. Around A, when motor decelerates and voltage drops, Tm + Pz exceeds Te + Pz, so motor accelerates and voltage rises. So A is a stable equilibrium expressing normal operation. By same fashion B is recognized as an unstable equilibrium, and C as stable equilibrium expressing stall, and character of Fig. 4.52 is preserved. Thus T-ω curve can be reflected as equivalent mapping onto P-V plane.

However referring Fig. 3, it must be noticed that P-V curve is equal to Te + Pz. Judge whether the equilibrium is stable or not, or the point means acceleration or deceleration are not is impossible. For the purpose Tm + Pz is needed, but Tm depends on ω and Pz depends on Vr. Here, ω and Vr is correspond one by one, so Tm + Pz was easily obtained.

Stability boundary curve[8][9]　First, "constant slip curve" that supports stability boundary theory is explained. This is a classic method but still used today[7]. The curve is plotted load's (or motor's) consumption power and voltage assuming ω does not vary. Assumed ω is constant, motor turns to constant impedance. The other parallel loads are also constant impedance. Therefore, constant slip curve is drawn as parabolic curve in P-V plane.

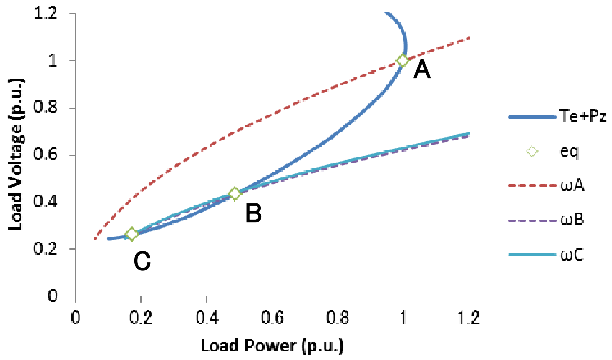

Fig. 4.54　Load's constant slip curve

Load's constant slip curves across the three equilibriums are drawn as Fig. 4.54. Lines across B and C seems almost piled up, but this is no more than accident.al affair.

Constant slip curve does not express Tm + Pz but expresses Te + Pz when speed w is constant. Therefore, mechanical torque Tm is not expressed anywhere in Fig. 4.45. Without grasping mechanical torque Tm, judging stability is impossible. To judge stability, motor's mechanical torque that varies by only speed ω must be taken into consideration.

As a method to bring motor's mechanical torque on P-V plane, "stability boundary curve" is presented. Motor is directly connected to voltage source Vr'. Mechanical torque balances to electric torque. Vr' is adjusted so that speed ω becomes equal to that in Fig.4.51 Therefore, motor's internal resistance Rm given by eq. (4.6) and mechanical torque given by eq. (4.10) also are equal to those in Fig. 4.51. Load consumption power is sum of mechanical torque Tm and impedance load' power Pz, and is expressed as a function of load voltage Vr'. The reason why load is directly connected to voltage source is the aim that "stability boundary is obtained by calculation independent from system side characteristics".

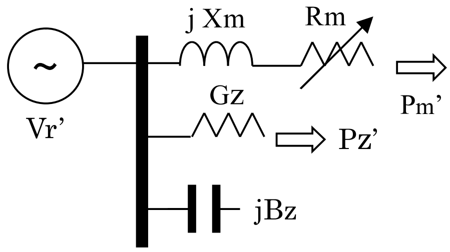

図 4.55 安定限界線のための系統モデル

In the method (Fig. 4.55) electric torque Te is balanced to mechanical torque Tm. On the contrary electric torque Te is not balanced to mechanical torque Tm (except at the three equilibrium) (Te≠Tm). Electric torque in the method is not equal to that of Fig. 4.51. So, electric torque of the method is expressed Te', that is, Te'≠Te.

Electric torque is decided as eq. (4.9) by load voltage Vr' and internal resistance Rm. Since internal resistance is same and electric torque is different (Te'≠Te), load voltage of the method Vr' is different from original system (Fig. 4.51), that is, Vr'≠Vr. Load voltage of the method Vr' can be obtaind from the condition that electric torque is balanced to mechanical torque as follows. .

$$\frac{Vr'^2\,Rm}{Rm^2 + Xm^2} = Te' = Tm = Tm_0\,\left(\frac{\omega}{\omega_0}\right)^2 \qquad (4.11)$$

Also, by load voltage changes to Vr' consumption power in resistance load of original system (Fig. 4.51) changes to Pz $(Vr'/Vr)^2$ or Gz Vr'^2. Therefore total load's consumption power is expressed as follows.

$$P_L' = \frac{Vr'^2\,Rm}{Rm^2 + Xm^2} + Gz\,Vr'^2 \qquad (4,12)$$

As the result of study above, on one hand "stability boundary curve" of the method is drawn as

Trajectory [Tm + Pz $(Vr'/Vr)^2$, Vr'] corresponding load voltage Vr'.

On the other hand, P-V curve that is also used in the method is same of Fig. 4.52 and 4.53, and is drawn as

Trajectory [Te + Pz, Vr] corresponding load voltage Vr.

The method draws these two trajectory on P-V plane having common power and voltage axis. (As to Vs and Vs' are mentioned after.) Since at the three equilibriums Vr' = Vr, stability boundary curve looks like Tm + Pz in Fig. 4.53 at a glance.

However generally, Vr' ≠Vr except at the three equilibriums, therefore minutely looking, stability boundary curve is different from the trajectory [Tm + Pz ,Vr] drawn in Fig. 4.53, and unreasonable issues as follows seems to appear.

1) New stable equilibrium D seems to appear between B and C.

2) C that was stable equilibrium seems to be an unstable equilibrium.

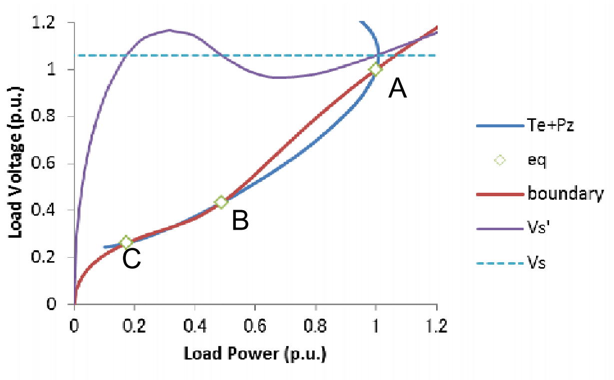

Fig. 4.56 Load's stability boundary curve (whole)

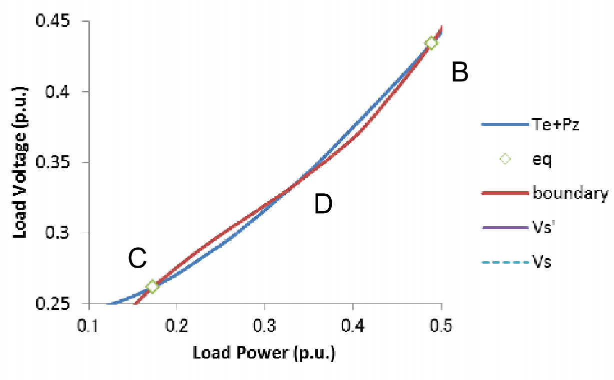

Fig. 4.57 Load's stability boundary curve (enlarged)

Here, it is demonstrated that these unreasonable issues are no more than appearance. For that at first, it is conducted that point on P-V curve at speed ω and point on stability boundary curve at speed ω locate on the same "equal slip curve". Here, it must be noticed that motor's internal resistance Rm takes the same value when speed ω is same.

Load's consumption power on "stability boundary curve" was conducted as eq. (4.12). Besides, load's consumption power P_L = Te + Pz is, joining resistance load's consumption power Pz = Gz Vr^2 to eq. (4.4), expressed as follows.

$$P_L = \frac{Vr^2\,Rm}{Rm^2 +} + Gz\,Vr^2 \qquad (4.13)$$

Equations (4.12) and (4.13) mean that point on P-V curve and point on "stability boundary curve" at speed ω, at which motor's internal resistance takes the same value Rm, locate on the same parabolic curve expressed by eq. (4.14). It must be noticed that the value in ( ) of the equation is constant. The parabolic curve is nothing but "equal slip curve" corresponding to speed ω (that is internal resistance Rm).

$$P = \left(\frac{Vr^2\,Rm}{Rm^2 + Xm^2} + Gz \right) V^2 \qquad (4.14)$$

As to point D, P-V curve and "stability boundary curve" are drawn by reducing speed ω from unstable equilibrium B as Fig. 4.58.

When speed is reduced to ω = 0.77936, tiptoe of P-V curve (Te + Pz) reaches poind D. But tiptoe of "stability boundary curve" is still locates right side over D (Dbnd). Since "stability boundary curve" expressing mechanical torque exceeds P-V curve expressing electric torque, the speed belongs to decelerating region.

When speed is reduced to ω = 0.72249, tiptoe of "stability boundary curve" reaches to point D. But tiptoe of P-V curve goes beyond D and locates left side under D (Dpv). Since "stability boundary curve" expressing mechanical torque exceeds P-V curve expressing electric torque, the speed also belongs to decelerating region.

Thus, both high speed side of D and low speed side of D belong to deceleration region, point D is not an equilibrium. However certainly, point D seems as if an equilibrium in Fig. 4.57. The appearance is derived from inadequate drawing that P-V curve and "stability boundary curve" having different voltage axes have drawn on the same P-V plane. Theory of "stability boundary curve" is never false.

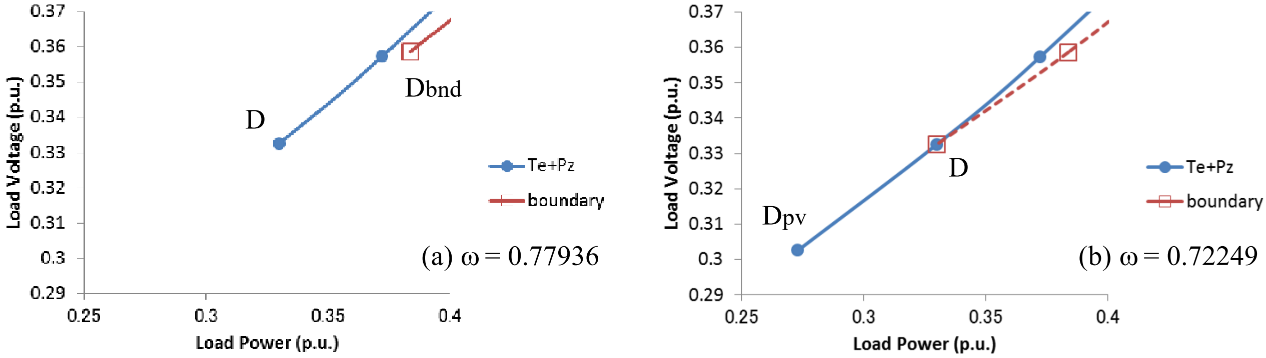

Fig. 4.58 Tiptoes of P-V curve and stability boundary curve

Next, as to point C, on "constant slip line" at slightly higher speed ω = 0.520 than C where ω = 0.512, point on "stability boundary curve" Cbnd$^+$ locates right side over point on P-V curve Cpv$^+$. Mechanical torque is superior to electric torque. Thus, those points belong to decelerating region.

On the contrary, on "constant slip line" at slightly lower speed ω = 0.500 than C where ω = 0.512, point on P-V curve Cpv$^-$ locates right side over point on "stability boundary curve" Cbnd$^-$. Electric torque is superior to mechanical torque. Thus, those points belong to accelerating region.

Since high speed side of C is decelerating region and low speed side of C is accelerating region, C is a stable equilibrium. Certainly C seems as if an unstable point in Fig. 4.57 at a glance, the appearance is derived from inadequate drawing of O-V curve and "stability boundary curve".

Thus, theory of "stability boundary curve" is never false, and the aim "calculated independent from system side character" has certainly some value, but some invention is needed in figure drawing.

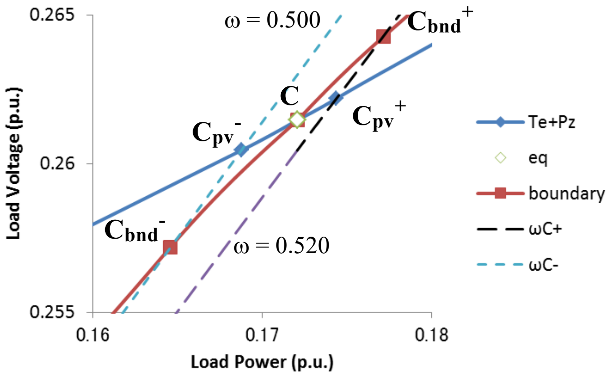

図 4.59 C 点の周りの P-V カーブと安定限界線

Giving common voltage axis[10] The two issues seemed as if unreasonable can be solved. For that, "stability boundary curve" is corrected to reflect mechanical torque at load voltage Vr instead of Vr'. In other words, "stability boundary curve" as

trajectory [Tm + Pz (Vr' / Vr)^2 , Vr']

is changed as

trajectory [Tm + Pz, Vr]

for having common voltage axis with P-V curve. Starting from "stability boundary curve", adding reasonable processing, the same result as Fig. 4.53 is obtained.

Fot that, infinite bus voltage Vs' that realizes in Fig. 4.51 the load voltage Vr', active and reactive load power P_L' and Q_L' in Fig. 4.55 is identified. At first, total load's reactive power Q_L' is calculated as follows, besides total load's active power P_L' already calculated in eq (4.12).

$$Q_L' = \frac{Vr'^2\,Xm}{Rm'^2 + Xm^2} - Bz\,Vr'^2 \qquad (4.15)$$

Load's current vector $\mathbf{I_L}$' is expressed as follows.

$$\mathbf{I_L}' = \frac{P_L' - j\, Q_L'}{Vr'} \qquad (4.16)$$

Infinite bus voltage vector **Vs'** is expressed as follows.

$$\mathbf{Vs}' = Vr' + j\, Xs\, \mathbf{I_L}' \qquad (4.17)$$

Magnitude of **Vs'** vector does not agree with Vs. Both are also drawn in Fig. 4.56. They agree only in load power corresponding the three equilibrium.

Here, maintaining motor speed ω (that is, slip s, internal resistance Rm, and mechanical torque Tm are maintained.), Vs' in Fig. 4.56 is changed to Vs as follows. Since slip s is maintained, motor becomes constant impedance, and total load also become constant impedance. As the result, relationship as follows exists between Vs, Vs', Vr, and Vr'.

$$\frac{Vr'}{Vr} = \frac{Vs'}{Vs} \qquad (4.18)$$

Therefore, accompanied with change from Vs' to Vs, Vr' is changed to Vr. By the process, mechanical torque Tm is corresponded not to Vr' but to Vr. Also, impedance load's consumption power becomes Pz. Thus "corrected stability boundary curve" is obtained as

trajectory [Tm + Pz, Vr].

Through more complicated calculation process, "corrected stability boundary curve (correct)" is drawn as Fig. 4.60, and unreasonable two issues of "stability boundary curve" are solved. In the figure, Tm + Pz in Fig. 4.53 is also drawn. The line just piles on "corrected stability boundary curve". Thus anticipated result is obtained, and it is verified again that theory of "stability boundary curve" is not false, and appearance of the two unreasonable issues is no more than a problem in figure drawing.

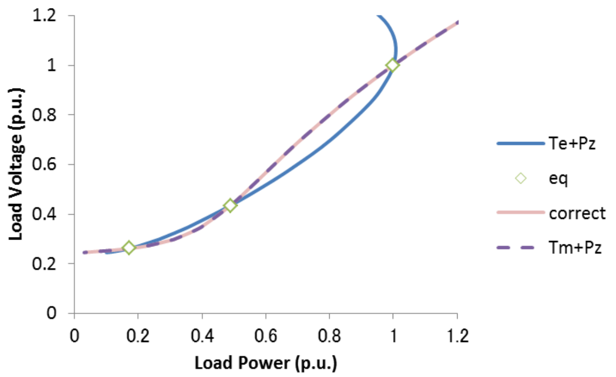

Fig. 4.60 corrected stability boundary curve

Simulation By T-ω curve theory, when once motor speed becomes slower than unstable equilibrium B speed ω_B, motor goes to stall and cannot return to normal. The predicted phenomenon is reproduced by simulation using CRIEPI Y-method program. Since the program considers main flux change that is ignored in analysis, short circuit failure is not modeled here.

Table 4.2 Parameters of the induction motor

V_r	W_M	P_M	Q_M	M_M	ω_0
1.0	1.0	0.5	0.051	0.5sec	0.975

X_1	X_2	X_M	R_1	R_2
0.001	0.199	999.9	0.00001	0.04949

Parameters of motor is selected as Table 4.2. Primary resistance R_1 is very small, nearly all reactance of primary winding X_1 is joined to that of secondary winding X_2, and excitation reactance X_M is very large, so that difference between analysis before becomes small. Secondary winding resistance R_2 is set as initial speed ω_0 becomes 0.975. W_M is motor capacity (kVA), M_M is unit inertia constant.

As disturbance, system side reactance Xs in Fig. 4.51 is increased to 1.25Xs during 2.5 sec. Motor decelerates. Variation of load voltage Vr , motor active power P_M , motor reactive power Q_M , motor speed ω are shown in Fig. 4.61. Motor speed ω become less than B: ω_B = 0.866 between 1.05 sec and 1.10 sec.

Therefore, if 1.25Xs is returned to Xs at 1.05 sec, motor speed is a little higher than ω_B, and motor accelerates and returns to normal operation A. If 1.25Xs is returned to Xs at 1.10 sec, motor speed is a little lower than ω_B, and motor decelerates and go to stall. Simulation results of the two cases are shown in Fig. 4.62. In case of 1.05 sec (Tc = 1.05) voltage recovers. In case of 1.10 sec (Tc = 1.1) voltage declines toward collapse. Thus, T-ω curve theory is verified by simulation.

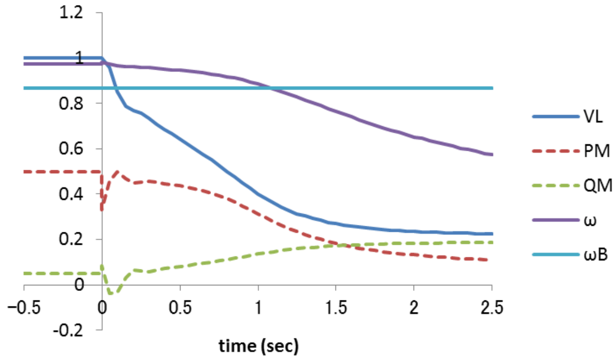

図 4.61 Xs の一時的増加による減速

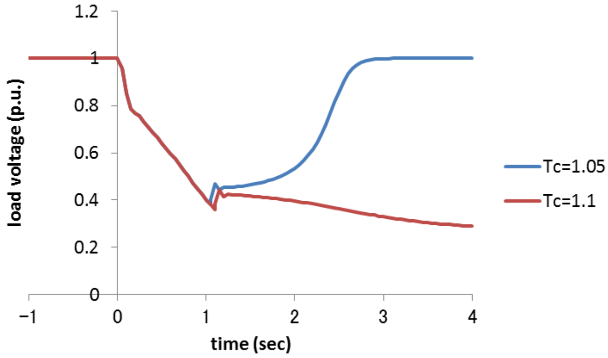

図 4.62 故障持続時間による負荷電圧の相違

As shown above, P-V curve corresponds to motor's electric torque, and "stability boundary curve" corresponds to motor's mechanical torque. The two theory explaining motor's stall phenomenon, that is, "T-ω curve" theory and "stability boundary curve" theory are equivalent. "T-ω curve" theory is already verified by simulation and experiment, "stability boundary curve" theory can also be used as reliable theory.

References

(1) T. Ueda and S. Komami: "Dynamic Load Stability in Bulk Power System with High DG Penetration", IEEJ Trans. PE, Vol. 127, No. 2, pp.371-378, (2007)

(2) T. Ueda and S. Komami: "Dynamic Load Model in Power System Based on Physical Structure and Measured Data", IEEJ Trans. PE, Vol. 126, No. 6, pp.635-823, (2006)

(3) M. Hosokawa, K. Kyogoku, K. Shinjo, and S. Komami: "Voltage Rise Mitigation and Energy Saving in Distribution Network by Combined Use of Light and Constant Leading Power Factor Operation of PVs and Vector-LDC Control of LTC", IEEJ Trans. PE, Vol. 135, No. 10, pp.583-590 (2015)

(4) K. Mizuo and S. Komami: "Parameter Identification Improvement of Dynamic Load Model in Power System", IEEJ Trans. PE, Vol. 132, No. 1, pp.71-76 (2012)

(5) NERC: "Fault-Induced Delayed Voltage Recovery" (2008)

(6) T. Ueda and S. Komami: "Experimental Evaluation of DG's Dynamic Voltage Support Capability Improving Short-Term Voltage Stability on Power System Loads", IEEJ Trans. PE, Vol. 128, No. 5, pp.761-768, (2008)

(7) K. Ishikawa, H. Taniguchi, H. Suzuki, Y. Ota, and Y. Mizuno:"Fundamental Study on Voltage Stability in Power System with Large Penetration of Photovoltaic Generation Considering Induction Motor Dynamics", IEEJ Trans. PE, Vol. 134, No. 7 号, pp.568-578 (2014)

(8) Kawabe, Tanaka: "Stability Boundary on P-V Plane for Analysis of Transient Voltage Stability", IEEJ Proc. PE, No. PE-13-111, pp.5-10 (2013)

(9) Kawabe , Tanaka: "Analytical Method for Short-Term Voltage Stability Using the Stability Boundary in the P-V Plane", IEEE Trans. on PS, Vol. 29, No. 6, pp.3041-3047, 2014

(10) S. Komami, S. Yamada, and T. Tanikawa,: "Equivalence of T-ω Curve and Stability Boundary Curve on Induction Motor Load's Stall Phenomenon", to be published in IEEJ Trans. PE, Vol. 137, No. 12, pp.???-??? (2017)